

Unique Four-electron Metal-to-Cage Charge Transfer of Th to a C₈₂ Fullerene Cage: Complete Structural Characterization of Th@C_{3v}(8)-C₈₂

Yaofeng Wang,^[a] Roser Morales-Martínez,^[b] Xingxing Zhang,^[a] Wei Yang,^[a] Yaxing Wang,^[d] Antonio Rodríguez-Forteza,^{*[b]} Josep M. Poblet,^[b] Lai Feng,^{*[c]} Shuao Wang,^{*[d]} and Ning Chen^{*[a]}

[a] Laboratory of Advanced Optoelectronic Materials, College of Chemistry, Chemical Engineering and Materials Science, Soochow University, Suzhou, Jiangsu, 215123 (P.R. China)

[b] Departament de Química Física i Inorgànica, Universitat Rovira i Virgili, c/Marcel·lí Domingo 1, 43007 Tarragona, (Spain)

[c] College of Physics, Optoelectronics and Energy & Collaborative, Innovation Center of Suzhou Nano Science and Technology, Soochow University, Suzhou, Jiangsu, 215006, (P.R. China)

[d] School of Radiological and Interdisciplinary Sciences & Collaborative Innovation Center of Radiation Medicine of Jiangsu, Higher Education Institutions, Soochow University, Suzhou, Jiangsu, 215123 (P.R. China)

KEYWORDS: actinides • fullerenes • photoluminescence • thorium • X-ray diffraction

ABSTRACT: Endohedral metallofullerenes (EMFs) containing lanthanides have been intensively studied in recent years. By contrast, actinide endohedral fullerenes remain largely unexplored. Herein, for the first time, we report the single crystal structure and full characterization of an actinide endohedral fullerene, Th@C₈₂, which exhibits remarkably different electronic and spectroscopic properties compared to those of lanthanide EMFs. Single crystal X-ray crystallography unambiguously established the molecular structure as Th@C_{3v}(8)-C₈₂. Combined experimental and theoretical studies reveal that Th@C_{3v}(8)-C₈₂ is the first example of an isolated monometallofullerene with four electrons transferred from the metal to the cage, with a surprisingly large electrochemical bandgap of 1.51 eV. Moreover, Th@C_{3v}(8)-C₈₂ displays a strong vibrationally coupled photoluminescence signal in the visible region, an extremely rare feature for both fullerenes and thorium compounds.

1. INTRODUCTION

Endohedral metallofullerenes (EMFs) have been extensively studied as promising materials in recent years.¹⁻³ These compounds feature both variable size and isomeric carbon cages and tunable electronic and magnetic properties which result from the nature of the encapsulated species.⁴⁻⁷ Up to now, except for a few cases, work in this field has mostly focused on the lanthanide based EMFs, given their relatively easy synthesis and high product yield.^{2,8-11} Early actinides from thorium to curium, which possess much richer valence states and more complicated electronic structures compared to their lanthanide analogues, have also been encapsulated into fullerene cages, motivated by their potential application in the field of nuclear medicine.^{12,13} Moreover, recent computational studies predicted unexpected actinide metal-metal bonds and unique cage structures for uranium-based EMFs, a rare feature that can only be observed in the gas phase.¹⁴⁻¹⁷ This suggests that EMFs may be an ideal platform to study the nature of bonding between actinides and ligands in condensed phases, in the absence of solvation effects.^{17,18} However, experimental studies of actinide EMFs are very rare: only a few mass and spectroscopic studies have been reported.¹⁹⁻²³ The molecular structures and physicochemical properties of actinide EMFs remain completely unknown to date. Herein, we present a complete and systematic study of an actinide EMF, Th@C_{3v}(8)-C₈₂. For

the first time, the molecular structure of an actinide EMF is disclosed from X-ray crystallographic analysis. A combined theoretical and experimental study revealed unprecedented features of Th@C_{3v}(8)-C₈₂, which are significantly different from those of lanthanide EMFs.

2. RESULTS AND DISCUSSION

Isolation and Characterizations of Th@C_{3v}(8)-C₈₂. The Th@C_{2n} (n=37-48) family was synthesized by a modified arc discharge method.²⁴ Graphite rods, packed with ThO₂ and graphite powder, were vaporized in the arcing chamber under He atmosphere. The resulting soot was then extracted with chlorobenzene. The mass spectrum of an as-extracted solution of the fullerene mixture (Figure 1(a)) shows that a large family of Th based metallofullerenes with multiple cages was generated during the arcing process, along with the empty fullerenes C_{2n}(n=48-59). The most abundant species, as indicated by Figure 1(a), is Th@C₈₂, followed by Th@C₈₆ and Th@C₇₆. A multistage HPLC procedure was employed to isolate and purify Th@C₈₂ (Figure S1). The purity of the isolated Th@C₈₂ was confirmed by HPLC (Figure 1b). The MALDI-TOF spectrum shows a peak at m/z 1216.050, corresponding to the mass of Th@C₈₂ and the observed isotopic distribution agrees well with the theoretical calculation (Figure 1c).

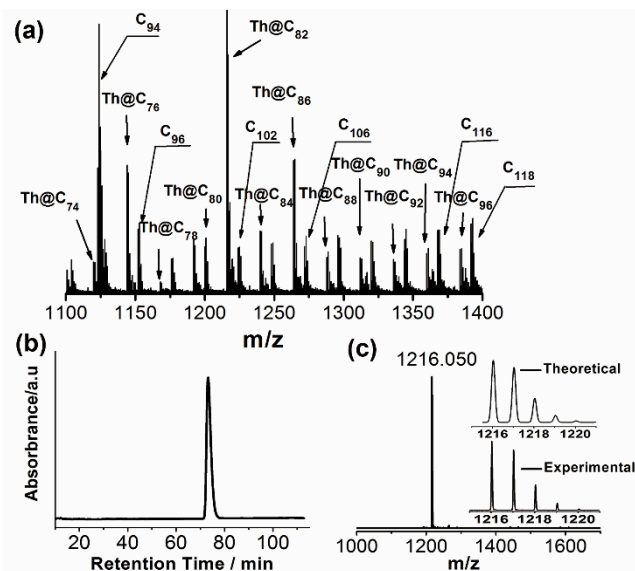


Figure 1. (a) Positive-ion mode MALDI-TOF mass spectrum of the as-extracted fullerene mixture. (b) HPLC chromatogram of the Th@C₈₂; using a 10 mm×250 mm Buckyprep column; flow rate 4.0 mL/min; toluene as moving phase. (c) Positive-ion mode MALDI-TOF mass spectrum of the purified Th@C₈₂. The inset shows the experimental and theoretical isotopic distribution for Th@C₈₂.

The unambiguous structure of Th@C₈₂ was determined by X-ray crystallography. The black block crystals of Th@C₈₂•[Ni^{II}(OEP)] were obtained by slow diffusion of a benzene solution of [Ni^{II}(OEP)] into a CS₂ solution of Th@C₈₂. Typically, a host-guest interaction can be observed between the fullerene and the [Ni^{II}(OEP)] moiety. A fully ordered C_{3v}(8)-C₈₂ cage was identified and represents the first example in which a single metal ion is encapsulated inside a C_{3v}(8)-C₈₂.² There is disorder in the position of the endohedral thorium ion. Only the major thorium site (i.e., Th1 with occupancy of 0.300(5) relative to the cage occupancy of 0.5) and its interaction with the closest cage portion carbons are shown in Figure 2. It is clearly seen that the Th1 site lies over a cage-carbon at the intersection of three hexagons (i.e., C15E) with a short Th-C distance of 2.340(14) Å, which is very close to the DFT-calculated value (see below discussion), indicating the favored position of the endohedral thorium ion. The short Th-cage contacts also occur between Th1 and cage carbons C03E, C14E and C16E with the distances ranging from 2.411(9) to 2.494(10) Å, suggesting a significant metal-cage interaction. Note that such a Th···C orientation is very different from that observed for conventional (C₅Me₅)₃ThH or (C₅Me₅)₂ThX₂ complexes, in which the metal is centered over the cyclopentadienide ring with a Th-(ring centroid) distance of around 2.5 Å.²⁵⁻²⁷ The metal···cage orientation in Th@C₈₂ is also unlike that observed for the majority of lanthanide EMFs (i.e., M@C_{2v}(9)-C₈₂, M=La, Ce, Gd, Sm, ect.),^{2,28-34} in which the endohedral metal is residing under a hexagon. Moreover, as a useful comparison, the Th-C distances are noticeably shorter than the Gd-C distances (2.515 and 2.523 Å) in Gd@C_{2v}(9)-C₈₂, though the ionic radius of Th⁴⁺ (0.94 Å) is almost identical to that of Gd³⁺ (0.94 Å).³⁵ This indicates that the metal-cage interaction in Th@C₈₂ is stronger than those for the lan-

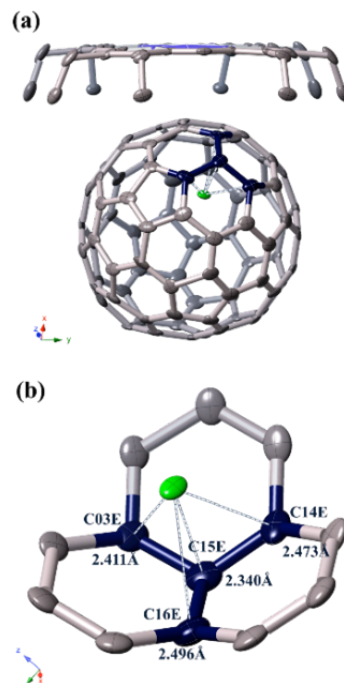


Figure 2. (a) Ortep drawing of Th@C_{3v}(8)-C₈₂•[Ni^{II}(OEP)] with 15% thermal ellipsoids, showing the relationship between the fullerene cage and [Ni^{II}(OEP)]. Only the major thorium site (Th1 with 0.300(5) occupancy) is shown. For clarity, the solvent molecules and minor metal sites are omitted. (b) The view showing the interaction of the metal ion (major metal site) with the closest cage portion.

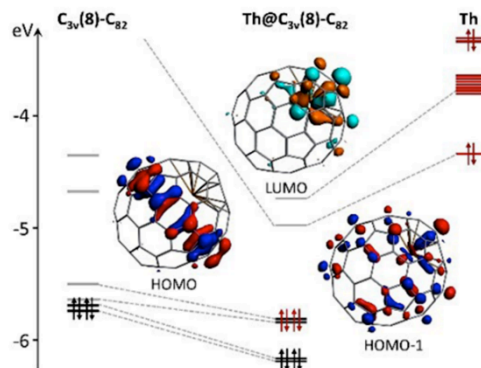


Figure 3. Orbital interaction diagram for Th@C_{3v}(8)-C₈₂. The C₈₂ fragment is calculated with the geometry that it has in the metallofullerene.

thanide counterparts. Three additional thorium sites with minor occupancies (i.e., 0.131(4) for Th2, 0.032(2) for Th3 and Th4, respectively) were identified inside the C_{3v}(8)-C₈₂ cage. It is interesting to note that all the identified thorium sites (i.e., Th1-Th4) are contained within a plane which is almost parallel to the adjacent [Ni^{II}(OEP)]. Such a metal-site distribution is again very different from other reported EMFs with the same cages i.e. Er₂@C_{3v}(8)-C₈₂³⁶ and Sc₂S@C_{3v}(8)-C₈₂³⁷, where the metal ions are distributed along a band of ten contiguous hexagons.

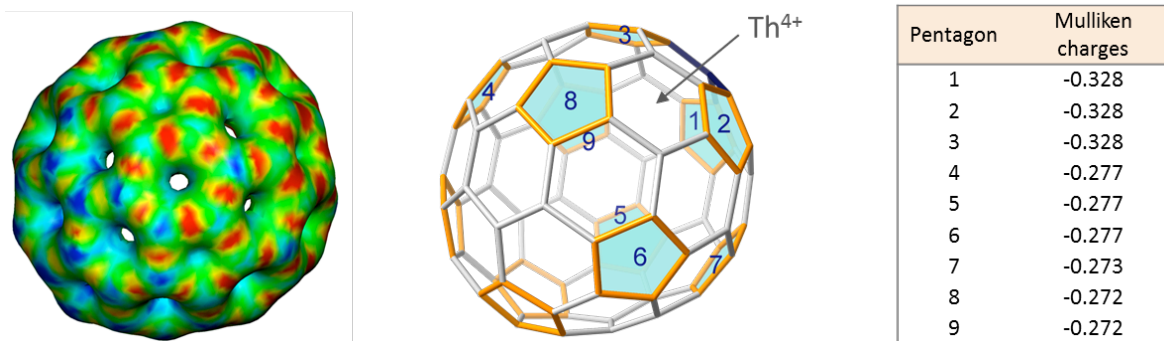


Figure 4. Molecular electrostatic potential distribution and Mulliken charges of the most charged pentagons of the tetraanionic $C_{3v}(8)-C_{82}$. Th^{4+} is placed near the most negatively charged environment.

From a detailed DFT analysis of the electronic structure of $Th@C_{3v}(8)-C_{82}$ (see SI for computational details), we have corroborated that there is an exceptional formal transfer of four electrons from the Th atom to the C_{82} cage, a situation never before observed for any isolated monometallofullerenes, except for the smallest observed systems, $M@C_{28}$ ($M = Ti, Zr, Hf$ and U), which have only been detected by high-resolution FT-ICR mass spectrometry.^{23,38} The four high-energy electrons of the Th atom are transferred to lower-lying unoccupied cage orbitals, with the metal remaining formally as a Th^{4+} ion (closed-shell f^0 configuration) and the cage as C_{82}^{4-} (see Figure 3). This formal transfer of four electrons is clearly confirmed by the lowest unoccupied orbitals that are mainly localized on the thorium center. As shown in Figure S3, there are six unoccupied molecular orbitals that are essentially atomic f Th orbitals (contributions between 50% and 70%). Besides, the LUMO and LUMO+12 show important contributions from Th (more than 35%). We have also computed the atomic charges according to the Bader partition and found a positive charge of +2.15 e for Th. The corresponding values for the La and Ba derivatives at the same level of theory were found to be +1.88 e and +1.61 e. This trend is in agreement with previous values reported for monometallic and clusterfullerenes with two, three and four electron formal transfers.³⁹ Below we show that the CV observed for $Th@C_{3v}(8)-C_{82}$, in particular the large electrochemical gap, is also in agreement with the formal four-electron transfer proposed here. It is important to keep in mind that even though Th-cage interaction can be easily described by the ionic model $Th^{4+}@C_{82}^{4-}$, non-negligible covalent interactions are also present, as can be inferred from the contribution of the Th orbitals to the frontier MOs (see for example HOMO-1 and LUMO in Figure 3).

We have selected the 9 isomers that satisfy the isolated pentagon rule (IPR) and the 75 non-IPR isomers with only one adjacent pentagon pair (APP1) of $Th@C_{82}$ to compute their energies (see SI). The lowest energy is found for isomer #8, which is close to that of isomer #9 (1.2 kcal mol⁻¹, see Table S2). The APP1 isomer #39705 has a much higher energy (37 kcal mol⁻¹). For $Th@C_{3v}(8)-C_{82}$, one position of the Th ion is significantly favoured with respect to the other ones (see Figure S5). This position is essentially the same as the one found with major occupancy factor by X-ray. In fact, the molecular electrostatic potential of $C_{3v}(8)-C_{82}^{4-}$ shows this region as the preferential one for the Th^{4+} ion to be maximally stabilized (see Figure 4). This unusual position of the Th atom at the intersection of three hexagons can be also understood consid-

-ering that the Th ion is interacting at the same time with the three most charged pentagons of the $C_{3v}(8)-C_{82}$ cage, which are symmetry equivalent (pentagons 1, 2 and 3 in Figure 4, which hold -0.328 e each), and far from the pyracylene motifs.⁴⁰ All the calculations for the $Th@C_{82}$ systems were made including relativistic corrections. The energy differences between isomers are essentially the same (within 0.1 kcal mol⁻¹) once the spin-orbit coupling is considered (see SI). Finally, in order to incorporate the effect of the high temperatures at which fullerenes are formed, we have computed the molar fractions of the lowest-energy isomers as a function of temperature. The rigid rotor and harmonic oscillator (RRHO) approximation predicts $Th@C_{3v}(8)-C_{82}$ as the most abundant isomer for the whole temperature range (see Figure S10), in good agreement with X-ray crystallographic experiments.

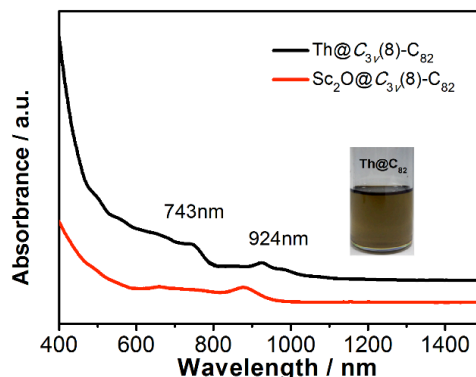


Figure 5. UV-vis-NIR absorption spectrum of $Th@C_{3v}(8)-C_{82}$ and $Sc_2O@C_{3v}(8)-C_{82}$ in CS_2 solution. The inset shows the photograph of $Th@C_{3v}(8)-C_{82}$ dissolved in CS_2 .

The purified $Th@C_{3v}(8)-C_{82}$ was investigated with UV-vis-NIR absorption spectroscopy. As Figure 5 shows, one characteristic sharp peak at 924 nm and a minor absorption peak at 743 nm were observed. The UV-vis-NIR absorption spectra of EMFs typically reflect the carbon cage symmetry and the charge distribution.^{2,11} The abovementioned features of $Th@C_{82}$ are substantially different from those of the previously reported lanthanide EMFs, which again, indicates a major difference on the metal-cage charge transfer or cage symmetry. Interestingly, these absorption features are similar to those of the $(Sc_2O)^{4+}@C_{3v}(8)-C_{82}^{4-}$, as shown in Figure 5, further suggesting an identical cage symmetry and charge transfer.⁴² Moreover, the absorption onset of the $Th@C_{3v}(8)-C_{82}$ is ~ 1120

Table 1. Redox potentials (V vs Fc^+/Fc) for the $\text{Th}@C_{3v}(8)\text{-C}_{82}$, $\text{Sc}_2\text{S}@C_{3v}(8)\text{-C}_{82}$, $\text{La}@C_{82}$, $\text{Sc}@C_{2v}(9)\text{-C}_{82}$ obtained in $(n\text{-Bu})_4\text{NPF}_6/o\text{-DCB}$ with ferrocene (Fc) as the internal standard. Computed values in square brackets.

compound	$E^{+/0}$	$E^{0/-}$	$E^{-2/}$	$E^{2-/3-}$	$E^{3-/4-}$	$E^{4-/5-}$	$E_{\text{gap,ec}}(\text{V})$	ref
$\text{Th}@C_{3v}(8)\text{-C}_{82}$	+0.46 ^a [+0.40]	-1.05 ^b [-1.09]	-1.54 ^b	-1.69 ^b	-1.82 ^b	-2.15 ^b	1.51 [1.49]	this work computations
$\text{Sc}_2\text{S}@C_{3v}(8)\text{-C}_{82}$	+0.52 ^a	-1.04 ^b	-1.19 ^b	-1.63 ^b			1.56	37
$\text{La}@C_{82}$	+0.07 ^a	-0.42 ^a	-1.37 ^a	-1.53	-2.26		0.49	41
$\text{Sc}@C_{2v}(9)\text{-C}_{82}$	+0.15	-0.35	-1.29				0.50	29

^aHalf-wave potential (reversible redox process). ^bPeak potential (irreversible redox process)

nm, which results in a surprisingly large optical band gap of 1.11 eV, making $\text{Th}@C_{3v}(8)\text{-C}_{82}$ the only monometallofullerene with a very large bandgap (Table S4 listed bandgaps of the typical reported monometallofullerenes).

The ^{13}C NMR spectrum of $\text{Th}@C_{3v}(8)\text{-C}_{82}$ carbon disulfide solution was shown in Figure 6. 11 major ^{13}C NMR signals from $\text{Th}@C_{3v}(8)\text{-C}_{82}$ were obtained. These 11 NMR signals are in the chemical shift range of 128-148 ppm (detailed values listed in Table S3), which are in line with the 11 major ^{13}C signals observed for $\text{Sc}_2\text{C}_2@C_{3v}(8)\text{-C}_{82}$ in range of 134-145 ppm.^{43,44} The small difference between the chemical shift range might be due to the impact of different encapsulated species. Moreover, all the peak widths at half height were less than 1 Hz, which clearly indicates the diamagnetism of the sample, further confirms its closed-shell electronic structure and the four-electron metal-cage charge transfer.

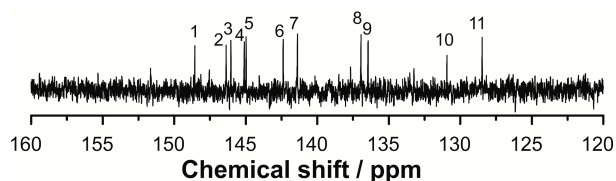


Figure 6. The ^{13}C NMR (150 MHz) spectrum of $\text{Th}@C_{3v}(8)\text{-C}_{82}$ (CS_2 , 298 K). A capillary tube containing acetone- d_6 was used as an internal lock.

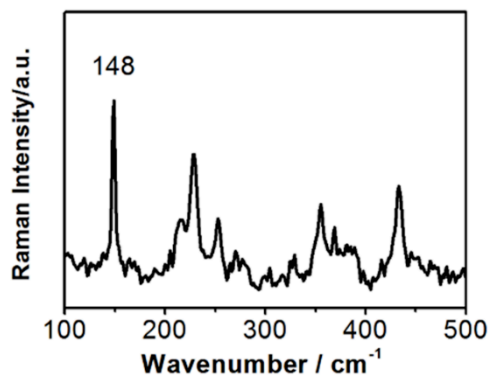


Figure 7. Low energy Raman spectrum of $\text{Th}@C_{3v}(8)\text{-C}_{82}$.

Figure 7 presents the low energy Raman spectrum of $\text{Th}@C_{3v}(8)\text{-C}_{82}$. Notably, an intense band was found at 148 cm^{-1} . The computational study assigns this band to the longitudinal metal-to-cage vibrational mode (see Figure S12), in line with previous reports that metal-to-cage vibrational frequency

in metallofullerenes occurs in the range of $150\text{-}200\text{ cm}^{-1}$.⁴⁵ A previous study suggests that the frequency of this mode could be defined as $\nu=(f/u)^{0.5}$, where f is the cluster-cage force constant and u is the reduced mass of M-C_{2n} system.⁴⁵ This frequency is very close to 140 cm^{-1} for $\text{Dy}^{3+}@C_{2v}(9)\text{-C}_{82}$.⁴⁶ Thus, with a similar vibration frequency and much larger mass for Th, the cluster-cage force constant for $\text{Th}@C_{3v}(8)\text{-C}_{82}$ must be much larger than that for $\text{Dy}^{3+}@C_{2v}(9)\text{-C}_{82}$,⁽⁵⁻⁾ as well as for the other lanthanide monometallofullerenes with three electron transfer. This result agrees well with the tetravalent electronic state of $\text{Th}^{4+}@C_{3v}(8)\text{-C}_{82}$.

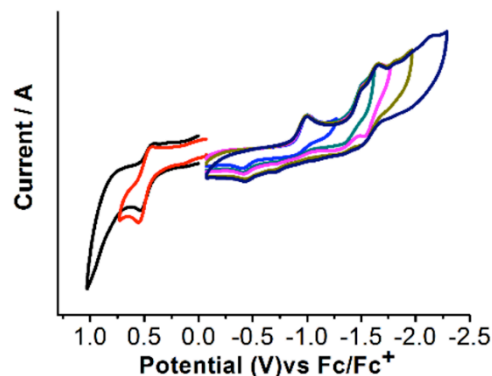


Figure 8. Cyclic voltammogram of $\text{Th}@C_{3v}(8)\text{-C}_{82}$ in o -dichlorobenzene (0.05 M $(n\text{-Bu})_4\text{NPF}_6$; scan rate 100 mV/s for CV).

The redox properties of $\text{Th}@C_{3v}(8)\text{-C}_{82}$, investigated by means of cyclic voltammetry (CV), again show major differences from the lanthanide metallofullerenes. To date, all the reported monometallofullerenes exhibit reversible reduction processes. The CV of $\text{Th}@C_{82}$, however, shows five irreversible reductive processes (Figure 8). Moreover, the first reduction and oxidation potential of $\text{Th}@C_{3v}(8)\text{-C}_{82}$ are at -1.05 V and 0.46 V , respectively, which is far more negative and positive than those of lanthanide monometallofullerenes, giving rise to an electrochemical bandgap of 1.51 eV, the largest among all the reported monometallofullerenes so far. This result correlates well with the large optical bandgap calculated by UV-vis-NIR absorption. Moreover, the computed first anodic and cathodic potentials for $\text{Th}@C_{3v}(8)\text{-C}_{82}$ compare very well with experiment (see Table 1), thus reproducing the rather large EC bandgap (theor. 1.49 V vs exp. 1.51 V), characteristic of the $C_{3v}(8)\text{-C}_{82}$ cage when formally accepting four electrons, as in $\text{Sc}_2\text{X}@C_{3v}(8)\text{-C}_{82}$ with $\text{X} = \text{O}, \text{S}$ or C_2 .^{42,47,48}

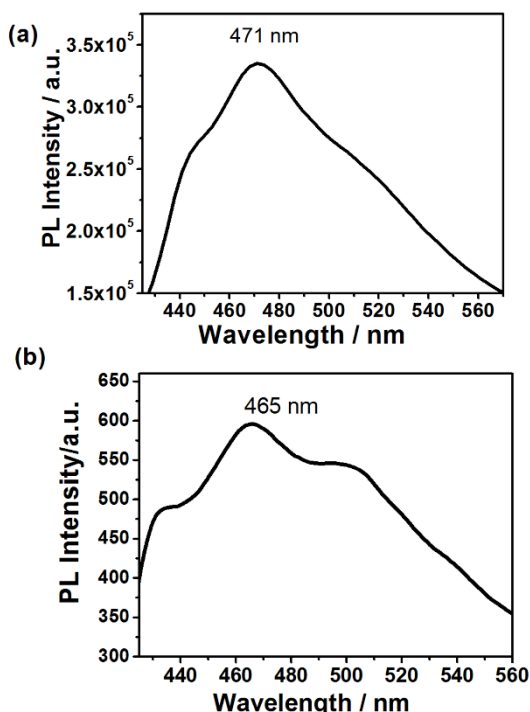


Figure 9: (a) PL spectrum of $\text{Th}@C_{3v}(8)\text{-C}_{82}$ in CS_2 solution upon excitation at 406 nm at room temperature. (b) PL spectrum of $\text{Th}@C_{3v}(8)\text{-C}_{82}$ solid powder upon excitation at 365 nm at room temperature.

Surprisingly, $\text{Th}@C_{3v}(8)\text{-C}_{82}$, both in CS_2 solution and in the solid state both display a strong photoluminescence (PL) emission. As shown in Figure 9, the solution PL spectrum of $\text{Th}@C_{3v}(8)\text{-C}_{82}$ presents signal centered at ca. 471 nm (2.63 eV), when excited under 406 nm UV light and the solid state PL spectrum also presents very similar emission. This phenomenon is extremely rare for either fullerene or for tetravalent thorium compounds. Photoluminescence has been rarely reported for either empty fullerenes or lanthanide EMFs. Although trivalent lanthanide ions are known to possess rich and distinct 4f-4f based photoluminescence properties, these signals can be efficiently quenched by the self-absorption from multiple electronic transition features of fullerenes. One possible reason is that all photoluminescence features for trivalent lanthanides are based on 4f-4f transitions, which are Laporte-forbidden originating from the selection rule. This leads to the fact that all trivalent lanthanide photoluminescence features are intrinsically weak that can be easily quenched. Only a near-IR luminescence of endohedral Er(III) could be detected corresponding to Er-based endohedral fullerenes.^{2,49} On the other hand, Th(IV) compounds are luminescence inactive given its $5f^0$ electron configuration. Note that the photoluminescence feature of $\text{Th}@C_{3v}(8)\text{-C}_{82}$ is significantly broad with the full width at half maximum of ca. 132 nm and vibrationally coupled, similar to the cases of luminescent uranyl compounds.⁵⁰ We therefore propose that the photoluminescence for $\text{Th}@C_{3v}(8)\text{-C}_{82}$ might originate from a charge transfer transition from the fullerene to a Th 6d orbital, which yields Th(III) and then emits by relaxing to a 5f configuration (orbitally-allowed transition with energy difference of 2.6 eV). Nevertheless, this transition seems to be exceptionally strong that

even the self-absorption of the fullerene cage cannot completely quench it, likely because compared to the trivalent lanthanide photoluminescence, the charge transfer based photoluminescence is intrinsically much brighter. This further highlights the substantially different bonding nature of the Th EMF from those in lanthanide EMFs. In addition, charge transfer photoluminescence has never been reported for Th(IV) compounds, likely because of the instability of Th(III) at the excited state. Thus, the photoluminescence observed for $\text{Th}@C_{3v}(8)\text{-C}_{82}$ suggests that Th(III) might be stabilized inside the fullerene cage, making the charge transfer based emission signals strong enough to be observable in both solution and solid state.

3. CONCLUSIONS

For the first time, an actinide endohedral fullerene, $\text{Th}@C_{82}$ has been successfully synthesized and fully characterized by mass spectrometry, single X-ray crystallography, UV-vis-NIR, ^{13}C NMR, cyclic voltammetry and photoluminescence spectroscopies. Crystallographic analysis unambiguously assigned the molecular structure to $\text{Th}@C_{3v}(8)\text{-C}_{82}$. Combined experimental and theoretical studies reveal that $\text{Th}@C_{3v}(8)\text{-C}_{82}$ is the first isolated metallofullerene with four electrons transferred from metal to the carbon cage, with a surprisingly large electrochemical bandgap of 1.51 eV. Moreover, $\text{Th}@C_{3v}(8)\text{-C}_{82}$ demonstrates a strong fluorescence in the UV-Vis range, unprecedented for both fullerene and thorium compounds. This work reveals that actinide EMFs have remarkably different structural and physical properties from those previously investigated lanthanide EMFs, which discloses the unique actinide behavior inside fullerene cage and opens a new frontier for the fullerene research.

4. EXPERIMENTAL METHODS

Synthesis and Isolation of $\text{Th}@C_{3v}(8)\text{-C}_{82}$. *Cautions!* ²³²Th ($T_{1/2} = 1.4 \times 10^{10}$ years) possesses health risk owing to an emission, and β and γ emissions from its daughters. Although the chemotoxicity and radiotoxicity of thorium are in general considered to be low, the standard procedure for handling radioactive materials should be followed. These experiments were conducted in a laboratory dedicated to studies on actinide elements. The carbon soot containing thorium metallofullerenes was synthesized by direct-current arc discharge method. The graphite rods, packed with ThO_2 powders and graphite powders (1:24 molar ratio), were vaporized in the arcing chamber under 300 Torr He atmosphere. The resulting soot was refluxed in chlorobenzene under an argon atmosphere for 12h. The separation and purification of $\text{Th}@C_{3v}(8)\text{-C}_{82}$ was achieved by a multistage HPLC procedure. Multiple HPLC columns, including Buckyprep M column (25×250 mm, Cosmosil, Nacalai Tesque Inc.), Buckyprep-D column (10×250mm, Cosmosil, Nacalai Tesque, Japan) and Buckyprep (10×250mm, Cosmosil, Nacalai Tesque, Japan), were utilized in this procedure. Further details are described in the Supporting Information.

Spectroscopic and Electrochemical Study. The positive-ion mode matrix-assisted laser desorption/ionization time-of-flight (Bruker, German) was employed for the mass characterization. UV-vis-NIR spectrum of the purified $\text{Th}@C_{3v}(8)\text{-C}_{82}$ was measured in CS_2 solution with a Cary 5000 UV-vis-NIR spectrophotometer (Agilent, U.S.A.). Raman spectrum was obtained on a Horiba LabRAM HR Evolution Raman spectrometer using a laser at 633 nm. Steady-state photoluminescence (PL)

spectra was recorded on FLS980 (Edinburgh Instrument, UK) with excitation at 406 nm at room temperature. PL spectrum of Th@C_{3v}(8)-C₈₂ solid powder were recorded upon excitation at 365 nm at room temperature with CRAIC 20/30 PVTM Microspectrophotometer.

¹³C NMR study. The Th@C_{3v}(8)-C₈₂ sample (ca.1.5 mg) was dissolved in CS₂ (0.8mL) and placed into a NMR tube. A capillary containing acetone-*d*₆ was used as an internal lock. The ¹³C NMR spectroscopic measurements were performed on 150 MHz with an Agilent Direct-Drive II 600 MHz spectrometer (Agilent, USA) at 298K. The total 239872 scans were recorded and the experimental time were 124.2 hrs.

Cyclic voltammetry (CV) and differential pulse voltammetry (DPV) were carried out in *o*-dichlorobenzene using a CHI-660E instrument. A conventional three-electrode cell consisting of a platinum counter-electrode, a glassy carbon working electrode, and a silver reference electrode was used for both measurements. (*n*-Bu)₄NPF₆ (0.05 M) as supporting electrolyte. The CV and DPV were measured at the scan rate of 100 mV/s and 20 mV/s, respectively.

X-ray Crystallographic Study. The black block crystals of Th@C₈₂•[Ni^{II}(OEP)] were obtained by slow diffusion of a CS₂ solution of Th@C₈₂ into a benzene solution of [Ni^{II}(OEP)]. X-ray data were collected at 173 K using a diffractometer (APEX II; Bruker Analytik GmbH) equipped with a CCD collector. Multiscan method was used for absorption correction. The structure was resolved using direct methods (SIR2004)⁵¹ and refined on F2 using full-matrix least-squares using SHELXL2013⁵² within the WinGX package.⁵³ Hydrogen atoms were inserted at calculated positions and constrained with isotropic thermal parameters.

Crystal data for Th@C_{3v}(8)-C₈₂•[Ni^{II}(OEP)]•1.5C₆H₆•CS₂: *M*_r=2001.61, 0.20×0.20×0.20 mm, monoclinic, *C* 2/*m* (No.12), *a*=27.1225(6), *b*=17.0996(5), *c*=17.6908(4), *α*=90, *β*=106.759(1), *γ*=90, *V*= 7856.2 (3) Å³, *Z*=4, *ρ*_{calcd}=1.692 g cm⁻³, *μ*(Cu_{Kα})=7.379 mm⁻¹, *θ*=3.094–68.373, *T*=173(2) K, *R*_F=0.0507, *wR*₂=0.1332 for all data; *R*₁=0.0479, *wR*₁=0.1300 for 6897 reflections (*I*> 2.0σ(*I*)) with 1053 parameters. Goodness of fit indicator 1.035. Maximum residual electron density 1.247 e Å⁻³. Crystallographic data has been deposited in the Cambridge Crystallographic Data Center (CCDC 1509968), which contains the supplementary crystallographic data for this paper.

ASSOCIATED CONTENT

Supporting Information.

The Supporting Information is available free of charge on the ACS Publications website.

HPLC profiles for the separation of Th@C_{3v}(8)-C₈₂, differential pulse voltammogram of Th@C_{3v}(8)-C₈₂ and computational details (PDF).

Additional crystal data for Th@C_{3v}(8)-C₈₂•[Ni^{II}(OEP)]•1.5C₆H₆•CS₂ (CIF).

¹³C NMR data file for Th@C_{3v}(8)-@C₈₂ (FID)

AUTHOR INFORMATION

Corresponding Author

*E-mail: chenning@suda.edu.cn

*E-mail: antonio.rodruiguez@urv.cat

*E-mail: fenglai@suda.edu.cn

*E-mail: shuaowang@suda.edu.cn.

Author Contributions

‡ Yaofeng Wang and Roser Morales-Martínez contributed equally to this work.

Notes

The authors declare no competing financial interest.

ACKNOWLEDGMENT

We cordially thank Prof. Xiaohong Li (Soochow University) for her kind help with the ¹³C NMR measurements and interpretation. This work is supported in part by the NSFC (51302178, 21422704, 21241004, 51372158 and 21305098), SRFDP (20123201120014), Jiangsu Specially Appointed Professor Program (SR10800113), Project for Jiangsu Scientific and Technological Innovation Team (2013), and Priority Academic Program Development of Jiangsu Higher Education Institutions (PAPD). This work was also supported by the Spanish Ministerio de Ciencia e Innovación (Project No. CTQ2014-52774-P) and by the Generalitat de Catalunya (2014SGR-199 and XRQTC). J.M.P. thanks the ICREA foundation for an ICREA ACADEMIA award. R.M. thanks the Spanish Ministerio de Ciencia e Innovación for a predoctoral fellowship.

REFERENCES

- (1) Bao, L.; Pan, C.; Slanina, Z.; Uhlik, F.; Akasaka, T.; Lu, X. *Angew. Chem. Int. Ed.*, **2016**, *55*, 9234-9238.
- (2) Popov, A. A.; Yang, S.; Dunsch, L. *Chem. Rev.*, **2013**, *113*, 5989-6113.
- (3) Junghans, K.; Schlesier, C.; Kostanyan, A.; Samoylova, N. A.; Deng, Q.; Rosenkranz, M.; Schiemenz, S.; Westerström, R.; Greber, T.; Büchner, B.; Popov, A. A. *Angew. Chem. Int. Ed.*, **2015**, *54*, 13411-13415.
- (4) Wu, B.; Wang, T.; Feng, Y.; Zhang, Z.; Jiang, L.; Wang, C. *Nat. Commun.*, **2015**, *6*, 6468.
- (5) Rodriguez-Forteza, A.; Balch, A. L.; Poblet, J. M. *Chem. Soc. Rev.*, **2011**, *40*, 3551-3563.
- (6) T.S. Wang, L. Feng, J.-Y. Wu, W. Xu, J.-F. Xiang, K. Tan, Y.-H. Ma, J.-P. Zheng, L. Jiang, X. Lu, C.-Y. Shu, C.-R. Wang, *J. Am. Chem. Soc.*, **2010**, *132*, 16362-16364
- (7) Liu, F.; Gao, C.-L.; Deng, Q.; Zhu, X.; Kostanyan, A.; Westerström, R.; Wang, S.; Tan, Y.-Z.; Tao, J.; Xie, S.-Y.; Popov, A. A.; Greber, T.; Yang, S. *J. Am. Chem. Soc.*, **2016**, *138*, 14764-14771.
- (8) Wei, T.; Wang, S.; Lu, X.; Tan, Y. Z.; Huang, J.; Liu, F. P.; Li, Q. X.; Xie, S. Y.; Yang, S. F. *J. Am. Chem. Soc.*, **2016**, *138*, 207-214.
- (9) Li, F. F.; Chen, N.; Mulet-Gas, M.; Triana, V.; Murillo, J.; Rodriguez-Forteza, A.; Poblet, J. M.; Echegoyen, L. *Chem. Sci.*, **2013**, *4*, 3404-3410.
- (10) Svitova, A. L.; Ghiassi, K. B.; Schlesier, C.; Junghans, K.; Zhang, Y.; Olmstead, M. M.; Balch, A. L.; Dunsch, L.; Popov, A. A. *Nat. Commun.*, **2014**, *5*, 3568.
- (11) Shinohara, H. *Rep. Prog. Phys.*, **2000**, *63*, 843-892.
- (12) Shultz, M. D.; Duchamp, J. C.; Wilson, J. D.; Shu, C.-Y.; Ge, J.; Zhang, J.; Gibson, H. W.; Fillmore, H. L.; Hirsch, J. I.; Dorn, H. C.; Fatouros, P. P. *J. Am. Chem. Soc.*, **2010**, *132*, 4980-4981.
- (13) Diener, M. D.; Alford, J. M.; Kennel, S. J.; Mirzadeh, S. *J. Am. Chem. Soc.*, **2007**, *129*, 5131-5138.
- (14) Foroutan-Nejad, C.; Vicha, J.; Marek, R.; Patzschke, M.; Straka, M. *Phys. Chem. Chem. Phys.*, **2015**, *17*, 24182-24192.
- (15) Dai, X.; Gao, Y.; Jiang, W. R.; Lei, Y. Y.; Wang, Z. G. *Phys. Chem. Chem. Phys.*, **2015**, *17*, 23308-23311.
- (16) Wu, X.; Lu, X. *J. Am. Chem. Soc.*, **2007**, *129*, 2171-2177.
- (17) Infante, I.; Gagliardi, L.; Scuseria, G. E. *J. Am. Chem. Soc.*, **2008**, *130*, 7459-7465.
- (18) Ryzhkov, M. V.; Ivanovskii, A. L.; Delley, B. *Comput. Theo. Chem.*, **2012**, *985*, 46-52.
- (19) Akiyama, K.; Sueki, K.; Haba, H.; Tsukada, K.; Asai, M.; Yaita, T.; Nagame, Y.; Kikuchi, K.; Katada, M.; Nakahara, H. *J. Radioanal. Nucl. Chem.*, **2003**, *255*, 155-158.

- (20) Guo, T.; Diener, M. D.; Chai, Y.; Alford, M. J.; Haufler, R. E.; McClure, S. M.; Ohno, T.; Weaver, J. H.; Scuseria, G. E.; Smalley, R. E. *Science*, **1992**, *257*, 1661-1664.
- (21) Diener, M. D.; Smith, C. A.; Veirs, D. K. *Chem. Mater.*, **1997**, *9*, 1773-1777.
- (22) Akiyama, K.; Zhao, Y.; Sueki, K.; Tsukada, K.; Haba, H.; Nagame, Y.; Kodama, T.; Suzuki, S.; Ohtsuki, T.; Sakaguchi, M.; Kikuchi, K.; Katada, M.; Nakahara, H. *J. Am. Chem. Soc.*, **2001**, *123*, 181-182.
- (23) Dunk, P. W.; Kaiser, N. K.; Mulet-Gas, M.; Rodríguez-Fortea, A.; Poblet, J. M.; Shinohara, H.; Hendrickson, C. L.; Marshall, A. G.; Kroto, H. W. *J. Am. Chem. Soc.*, **2012**, *134*, 9380-9389.
- (24) Kratschmer, W.; Lamb, L. D.; Fostiropoulos, K.; Huffman, D. R. *Nature* **1990**, *347*, 354-358.
- (25) Browne, K. P.; Maerzke, K. A.; Travia, N. E.; Morris, D. E.; Scott, B. L.; Henson, N. J.; Yang, P.; Kiplinger, J. L.; Veauthier, J. M. *Inorg. Chem.*, **2016**, *55*, 4941-4950.
- (26) Batrice, R. J.; Fridman, N.; Eisen, M. S. *Inorg. Chem.*, **2016**, *55*, 2998-3006.
- (27) Monreal, M. J.; Seaman, L. A.; Goff, G. S.; Michalczyk, R.; Morris, D. E.; Scott, B. L.; Kiplinger, J. L. *Angew. Chem. Int. Ed.*, **2016**, *55*, 3631-3636.
- (28) Sato, S.; Nikawa, H.; Seki, S.; Wang, L.; Luo, G.; Lu, J.; Haranaka, M.; Tsuchiya, T.; Nagase, S.; Akasaka, T. *Angew. Chem. Int. Ed.*, **2012**, *51*, 1589-1591.
- (29) Hachiyu, M.; Nikawa, H.; Mizorogi, N.; Tsuchiya, T.; Lu, X.; Akasaka, T. *J. Am. Chem. Soc.*, **2012**, *134*, 15550-15555.
- (30) Nikawa, H.; Yamada, T.; Cao, B.; Mizorogi, N.; Slanina, Z.; Tsuchiya, T.; Akasaka, T.; Yoza, K.; Nagase, S. *J. Am. Chem. Soc.*, **2009**, *131*, 10950-10954.
- (31) Lu, X.; Nikawa, H.; Feng, L.; Tsuchiya, T.; Maeda, Y.; Akasaka, T.; Mizorogi, N.; Slanina, Z.; Nagase, S. *J. Am. Chem. Soc.*, **2009**, *131*, 12066-12067.
- (32) Akasaka, T.; Kono, T.; Takematsu, Y.; Nikawa, H.; Nakahodo, T.; Wakahara, T.; Ishitsuka, M. O.; Tsuchiya, T.; Maeda, Y.; Liu, M. T.; Yoza, K.; Kato, T.; Yamamoto, K.; Mizorogi, N.; Slanina, Z.; Nagase, S. *J. Am. Chem. Soc.*, **2008**, *130*, 12840-12841.
- (33) Nikawa, H.; Kikuchi, T.; Wakahara, T.; Nakahodo, T.; Tsuchiya, T.; Rahman, G. M. A.; Akasaka, T.; Maeda, Y.; Yoza, K.; Horn, E.; Yamamoto, K.; Mizorogi, N.; Nagase, S. *J. Am. Chem. Soc.*, **2005**, *127*, 9684-9685.
- (34) Feng, L.; Nakahodo, T.; Wakahara, T.; Tsuchiya, T.; Maeda, Y.; Akasaka, T.; Kato, T.; Horn, E.; Yoza, K.; Mizorogi, N.; Nagase, S. *J. Am. Chem. Soc.*, **2005**, *127*, 17136-17137.
- (35) Suzuki, M.; Lu, X.; Sato, S.; Nikawa, H.; Mizorogi, N.; Slanina, Z.; Tsuchiya, T.; Nagase, S.; Akasaka, T. *Inorg. Chem.*, **2012**, *51*, 5270-5273.
- (36) Olmstead, M. M.; Lee, H. M.; Stevenson, S.; Dorn, H. C.; Balch, A. L. *Chem. Commun.*, **2002**, 2688-2689.
- (37) Mercado, B. Q.; Chen, N.; Rodríguez-Fortea, A.; Mackey, M. A.; Stevenson, S.; Echegoyen, L.; Poblet, J. M.; Olmstead, M. M.; Balch, A. L. *J. Am. Chem. Soc.*, **2011**, *133*, 6752-6760.
- (38) Munoz-Castro, A.; Bruce King, R. *J. comput. chem.*, **2017**, *38*, 44-50.
- (39) Rodríguez-Fortea A., Alegret N. and Poblet J.M. Endohedral Fullerenes. In: Jan Reedijk and Kenneth Poeppelmeier, editors. *Comprehensive Inorganic Chemistry II*, Vol 9. Oxford: Elsevier; 2013. p. 907-924.
- (40) Rodríguez-Fortea, A.; Alegret, N.; Balch, A. L.; Poblet, J. M. *Nat. Chem.*, **2010**, *2*, 955-961.
- (41) Suzuki, T.; Kikuchi, K.; Oguri, F.; Nakao, Y.; Suzuki, S.; Achiba, Y.; Yamamoto, K.; Funasaka, H.; Takahashi, T. *Tetrahedron* **1996**, *52*, 4973-4982.
- (42) Tang, Q.; Abella, L.; Hao, Y.; Li, X.; Wan, Y.; Rodríguez-Fortea, A.; Poblet, J. M.; Feng, L.; Chen, N. *Inorg. Chem.*, **2016**, *55*, 1926-1933.
- (43) E. Yamamoto, M. Tansho, T. Tomiyama, H. Shinohara, H. Kawahara and Y. Kobayashi, *J. Am. Chem. Soc.*, **1996**, *118*, 2293-2294.
- (44) Iiduka, Y.; Wakahara, T.; Nakajima, K.; Tsuchiya, T.; Nakahodo, T.; Maeda, Y.; Akasaka, T.; Mizorogi, N.; Nagase, S. *Chem. Commun.*, **2006**, 19,2057-2059.
- (45) Lebedkin, S.; Renker, B.; Heid, R.; Schober, H.; Rietschel, H. *Appl. Phys. A*, **1998**, *66*, 273-280.
- (46) Wågberg, T.; Launois, P.; Moret, R.; Huang, H. J.; Yang, S. H.; Li, I. L.; Tang, Z. K. *Eur. Phys. J. B*, **2003**, *35*, 371-375.
- (47) Chen, N.; Chaur, M. N.; Moore, C.; Pinzon, J. R.; Valencia, R.; Rodríguez-Fortea, A.; Poblet, J. M.; Echegoyen, L. *Chem. Commun.*, **2010**, *46*, 4818-4820.
- (48) Kurihara, H.; Lu, X.; Iiduka, Y.; Mizorogi, N.; Slanina, Z.; Tsuchiya, T.; Nagase, S.; Akasaka, T. *Chem. Commun.*, **2012**, *48*, 1290-1292.
- (49) Ito, Y.; Okazaki, T.; Okubo, S.; Akachi, M.; Ohno, Y.; Mizutani, T.; Nakamura, T.; Kitaura, R.; Sugai, T.; Shinohara, H. *ACS Nano* **2007**, *1*, 456-462.
- (50) Denning, R. G.; Norris, J. O. W.; Short, I. G.; Snellgrove, T. R.; Woodwark, D. R. in *Lanthanide and Actinide Chemistry and Spectroscopy*; Edelstein, N. M, Ed; ACS Symposium Series, Vol. 131; American Chemical Society: Washington, DC, 1980; Chapter 15.
- (51) Burla, M. C.; Caliandro, R.; Camalli, M.; Carrozzini, B.; Cascarano, G. L.; De Caro, L.; Giacovazzo, C.; Polidori, G.; Spagna, R. *J. Appl. Cryst.*, **2005**, *38*, 381-388.
- (52) Sheldrick, G. *Acta. Cryst. C*, **2015**, *71*, 3-8.
- (53) Farrugia, L. *J. Appl. Cryst.*, **2012**, *45*, 849-854.

TOC

